PHILOSOPHICAL TRANSACTIONS OF THE ROYAL SOCIETY A

Phil. Trans. R. Soc. A (2009) **367**, 2181–2202
doi:10.1098/rsta.2008.0304

Modelling sarcoplasmic reticulum calcium ATPase and its regulation in cardiac myocytes

By Jussi T. Koivumäki[1,2], Jouni Takalo[1,2], Topi Korhonen[2,3], Pasi Tavi[2,3] and Matti Weckström[1,2,*]

[1]*Division of Biophysics, Department of Physical Sciences,* [2]*Biocenter Oulu, and* [3]*Department of Physiology, Institute of Biomedicine, University of Oulu, 90014 Oulu, Finland*

When developing large-scale mathematical models of physiology, some reduction in complexity is necessarily required to maintain computational efficiency. A prime example of such an intricate cell is the cardiac myocyte. For the predictive power of the cardiomyocyte models, it is vital to accurately describe the calcium transport mechanisms, since they essentially link the electrical activation to contractility. The removal of calcium from the cytoplasm takes place mainly by the Na^+/Ca^{2+} exchanger, and the sarcoplasmic reticulum Ca^{2+} ATPase (SERCA). In the present study, we review the properties of SERCA, its frequency-dependent and β-adrenergic regulation, and the approaches of mathematical modelling that have been used to investigate its function. Furthermore, we present novel theoretical considerations that might prove useful for the elucidation of the role of SERCA in cardiac function, achieving a reduction in model complexity, but at the same time retaining the central aspects of its function. Our results indicate that to faithfully predict the physiological properties of SERCA, we should take into account the calcium-buffering effect and reversible function of the pump. This 'uncomplicated' modelling approach could be useful to other similar transport mechanisms as well.

Keywords: heart; calcium; sarcoplasmic reticulum Ca^{2+} ATPase; mathematical modelling

1. Calcium transport in cardiomyocytes: role of sarcoplasmic reticulum Ca^{2+} ATPase

In cardiac myocytes, the contraction force produced by the contractile apparatus is directly (albeit not linearly) related to the momentary calcium concentration in the cytoplasm. The continuous contraction–relaxation cycle, characteristic of heart function, is created by oscillation-like increases and decreases in calcium concentration, the Ca^{2+} transients. These arise from a complex chain of events, collectively known as excitation–contraction (E–C) coupling, which is paced by membrane action potentials (APs). During the cycle, Ca^{2+} flows into the

* Author and address for correspondence: Department of Physical Sciences, University of Oulu, PO Box 3000, 90014 Oulu, Finland (matti.weckstrom@oulu.fi).

One contribution of 15 to a Theme Issue 'The virtual physiological human: tools and applications II'.

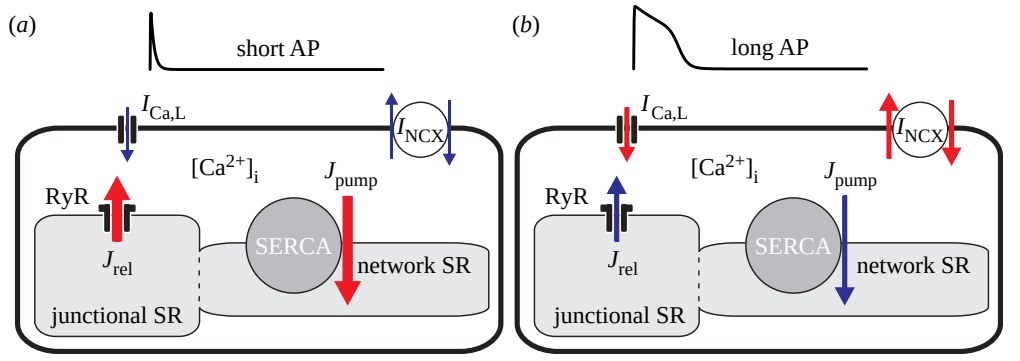

Figure 1. Calcium fluxes and balances. (*a*) In the myocytes of mammals with short APs, a majority (approx. 90% for mouse) of calcium is released from and recirculated back to sarcoplasmic reticulum (SR) via ryanodine receptor (RyR) channel and SR Ca^{2+} ATPase (SERCA). However, (*b*) in the case of animals with long APs, the contribution of trans-sarcolemmal calcium fluxes (L-type calcium current; $I_{Ca,L}$ and Na^+/Ca^{2+} exchange current; I_{NCX}) is almost equal (25–50%) to J_{pump}.

myocyte through (voltage-activated) L-type calcium channels and, triggered by the influx, additional calcium is released from intracellular stores (sarcoplasmic reticulum; SR), via calcium-activated release channels (ryanodine receptors) (Bers 2001). Removal of calcium from the cytosol, responsible for the mechanical relaxation, is caused by rapid transportation of the same amount of calcium from the cytoplasm by three different mechanisms: the sarcolemmal Ca^{2+} ATPase; the Na^+/Ca^{2+} exchanger (NCX); and the Ca^{2+} ATPase in the SR (SERCA) (for reviews see Blaustein & Lederer (1999), Cartwright *et al.* (2005) and Inesi *et al.* (2008), respectively). Of these, only the last two transport significant amounts during the calcium transient in ventricular myocytes (Bers 2001).

Rapid and efficient calcium removal is necessary for the normal functioning of cardiac myocytes, and compromised removal is one of the hallmarks of cardiac failure. In the present study, we briefly review the properties and physiological role of SERCA, with emphasis on its regulatory modulation and its mathematical modelling. The basic mechanisms have been reviewed at length (Koss & Kranias 1996; Bers 2002; MacLennan & Kranias 2003; Periasamy *et al.* 2008), including considerations of the properties of SERCA isoforms (Periasamy & Kalyanasundaram 2007) and the specific mode of its action, especially the role of calcium affinity (Vangheluwe *et al.* 2006). The availability of several transgenic animal models for investigating the calcium-handling proteins (Kiriazis & Kranias 2000; Sorrentino & Rizzuto 2001; Hiranandani *et al.* 2007) is an additional recent development, and the knowledge of those studies can also be used here. In the second part of the present work, we offer some novel theoretical considerations that may be used to understand the calcium transport function of SERCA that is so central to cardiac function.

(*a*) *Species-specific differences*

The relative importance of the NCX and the SERCA as calcium removers varies from species to species, depending roughly on the length of the AP (Barry & Nerbonne 1996; see figure 1 for illustration). During long APs (as in guinea-pigs and humans), the influx of calcium is relatively large, owing to the long time that the

L-type channels are at least moderately open (Linz & Meyer 2000; Han *et al.* 2002). The same amount has to be extruded via the NCX during each cycle in order to retain the balance and prevent accumulation of calcium either into the cytosol or into the SR. Thence the relative importance of the NCX is large likewise in long AP myocytes. In short AP myocytes (as in mice and rats), the release of calcium from the intracellular stores is larger, and the SERCA is relatively more important than that in long AP species (Bers 2001; Shannon *et al.* 2004).

SERCA exists in three (tissue-specific) subtypes 1–3. In this study, we focus on SERCA2, although many of the considerations are applicable for the other subtypes as well, since the main distinctive properties are affinity and maximum transport rate. Currently, no extensive quantitative data of the expression levels are available of the two main SERCA2 isoforms A and B in cardiac tissue of different species. These data would be very useful for comparing the observations made in the foetal or adult myocytes of various species in either normal or diseased heart, thus enabling a further linking of the data to pathophysiological states in human cardiology.

(*b*) *Thermodynamics of SERCA*

The function of SERCA is inherently regulated by the momentary changes of (free) concentration of Ca^{2+} in the cytoplasm on the one hand and the amount of free calcium inside the SR on the other. These concentrations have a dual importance: the Ca^{2+} affinities of SERCA on either side have an obvious effect on its function, while the SERCA is a bidirectional pump, but the concentrations also affect its thermodynamics. With a stoichiometry of two Ca^{2+} ions moved per ATP hydrolysed, and assuming no other factors (such as counter-ion transport), SERCA is able to produce a 1 : 7000 calcium gradient, cytoplasm : SR, correspondingly (Shannon & Bers 1997). There is ample evidence that the SERCA transports two H^+ ions from the SR to the cytoplasm in neutral pH (Kuhlbrandt 2004; Niggli & Sigel 2008). Therefore, it is not only electrogenic but also coupled to pH on both cytoplasm and SR lumen. Thereby, the thermodynamics becomes more complicated, but while the thermodynamic limits are never achieved during normal cycling operation of the pump, we can safely use the uniport concept of SERCA in physiological modelling, still keeping in mind its more complex operation.

(*c*) *Regulation of SERCA*

The importance of SERCA is emphasized by the fact that the amount of calcium stored in SR depends solely on its balancing action, restoring the calcium released during each cycle. The SERCA is able to do this under changing circumstances because it is regulated via an inhibitory protein, phospholamban (PLB). This can be phosphorylated by protein kinase A (PKA; A-type kinase, activated by the β-adrenergic pathway via cyclic adenosire monophosphate), which leads to phosphorylation at the Ser16 site (Chu *et al.* 2000). Independent of this, another enzyme, calcium/calmodulin-dependent kinase type II (CaMKII), acts at the Thr17 site of PLB, and this effect, while it depends on CaMKII becoming activated by calcium, depends on the beating frequency (Hagemann *et al.* 2000). Once phosphorylated, the inhibition is released, and the calcium pumping action is enhanced.

Obviously, the molar ratio of PLB to SERCA can be conceived as a critical determinant of the contraction force and its regulation (Koss *et al.* 1997; Meyer *et al.* 1999). This fact constitutes a strong negative feedback loop in the internal circulation of calcium which is potentially unstable (Diaz *et al.* 2005). A further complication in the regulation of SERCA is that CaMKII is able to directly activate it by direct phosphorylation (of Ser38 or SERCA; Toyofuku *et al.* 1994; Xu & Narayanan 1999).

2. Approaches for modelling the function of SERCA

The direct measurement of the calcium flux produced by SERCA (either uni- or bidirectional) is not possible in intact myocytes. However, several factors defining the calcium fluxes can be fairly reliably estimated. These include the determination of SR calcium content (or the 'releasable pool' of calcium), total amount of calcium increase during a cycle (the 'integral' of the calcium transient) and the flux through the NCX, to name a few. Hence, the SERCA function is always, even in experimental studies, the result of derivation or calculation, including possibly the errors and experimental variation of several physiological functions. The modelling of SERCA offers supplementary information, with which interpretations of experimental studies can be tested. An additional benefit of modelling is that it offers possibilities to do experiments not feasible in real cells. Lastly, testing of the function of genetically modified myocytes is possible *in silico*.

Owing to the prominent role of SERCA in the regulation of cellular calcium dynamics, it has been included in mathematical cell models ever since the fundamental studies of DiFrancesco & Noble (1985) and Luo & Rudy (1994). In cardiomyocyte models, the Ca^{2+} uptake to the SR via SERCA has been traditionally modelled with a unidirectional pump that is activated by the increase in the cytosolic calcium concentration (Luo & Rudy 1994; Jafri *et al.* 1998; Bondarenko *et al.* 2004). During recent years, more complicated models, which take into account also the effect of SR calcium concentration and the calcium-buffering/binding effect of SERCA, have been developed. In the following subsections, we will review the pros and cons of the previously published approaches for the modelling of calcium transport by SERCA and its phosphorylatory regulation.

(*a*) *Unidirectional pump model*

Based on the simplifying assumption that calcium transport takes place only from the cytoplasm to the SR and that it behaves as first-order enzyme kinetics, the basic Hill equation has been used to define a unidirectional model of the SERCA (Luo & Rudy 1994; Jafri *et al.* 1998; Bondarenko *et al.* 2004):

$$J_{\mathrm{pump}} = V_{\max} \frac{[Ca^{2+}]_i^2}{EC_{50}^2 + [Ca^{2+}]_i^2}, \tag{2.1}$$

where $V_{\max}$ is the maximum pump current; $[Ca^{2+}]_i$ is the cytosolic calcium concentration; and EC_{50} is the concentration at which a half-maximal uptake is observed, which is approximately 0.3 μM for mammalian myocytes (Bers 2001).

Until recently, most mathematical models of intracellular calcium dynamics have used this model. It has the obvious advantage of simplicity. However, the assumption that the pumping activity depends exclusively on the cytosolic calcium concentration is not accurate on the basis of experimental results (Favre *et al.* 1996; Shannon *et al.* 2000, 2001). According to the unidirectional model, SERCA would still be able to pump calcium to the SR, although the diastolic calcium concentration were low, when in fact this would be largely stopped by the large concentration gradient across the SR. This unwanted feature of SERCA modelling has to be balanced in whole myocyte models with an artefactually large SR calcium leak from the SR to cytosol, introducing a 'futile' cycling of calcium into the myocyte models.

(*b*) *Pump models accounting for the effect of SR calcium*

The first mathematical description of the dependence of SERCA on SR calcium concentration was proposed by Favre *et al.* (1996). Based on the measurement with cell homogenates, they reported a supralinear feedback inhibition of Ca^{2+} uptake by the Ca^{2+} load of intracellular stores, which led them to use the form of logistic equation for SERCA. These findings were simplified for a whole-cell mathematical model by Sneyd *et al.* (2003), who formulated an equation where calcium uptake is inversely related to SR calcium concentration (see equation (2.1) to compare):

$$J_{\mathrm{pump}} = V_{\max} \frac{[\mathrm{Ca}^{2+}]_{\mathrm{i}}}{\mathrm{EC}_{50} + [\mathrm{Ca}^{2+}]_{\mathrm{i}}} \frac{1}{[\mathrm{Ca}^{2+}]_{\mathrm{SR}}}, \tag{2.2}$$

where $V_{\max}$ is the maximum pump current; $[\mathrm{Ca}^{2+}]_{\mathrm{i}}$ is the cytosolic calcium concentration; $[\mathrm{Ca}^{2+}]_{\mathrm{SR}}$ is the SR calcium concentration; and EC_{50} is the concentration at which a half-maximal uptake is observed. While introducing a major improvement, this pump model still has a fundamental limitation: the pump flux tends to zero only in non-realistic conditions, in which either $[\mathrm{Ca}^{2+}]_{\mathrm{i}}=0$ or $[\mathrm{Ca}^{2+}]_{\mathrm{SR}}=\infty$.

This problem can be solved by assuming that the net pump flux consists of the sum of separate forward and reverse modes (Shannon *et al.* 2000):

$$J_{\mathrm{pump}} = \frac{V_{\max}\left(\left(\dfrac{[\mathrm{Ca}^{2+}]_{\mathrm{i}}}{\mathrm{EC}_{50}^{\mathrm{fwd}}}\right)^2 - \left(\dfrac{[\mathrm{Ca}^{2+}]_{\mathrm{SR}}}{\mathrm{EC}_{50}^{\mathrm{rev}}}\right)^2\right)}{1 + \left(\dfrac{[\mathrm{Ca}^{2+}]_{\mathrm{i}}}{\mathrm{EC}_{50}^{\mathrm{fwd}}}\right)^2 + \left(\dfrac{[\mathrm{Ca}^{2+}]_{\mathrm{SR}}}{\mathrm{EC}_{50}^{\mathrm{rev}}}\right)^2}, \tag{2.3}$$

where $V_{\max}$ is the maximum pump current; $[\mathrm{Ca}^{2+}]_{\mathrm{i}}$ is the cytosolic calcium concentration; $[\mathrm{Ca}^{2+}]_{\mathrm{SR}}$ is the calcium concentration in the SR; and EC_{50} is the concentration at which a half-maximal flux is observed, either in the forward (fwd) or in the reverse (rev) direction. In addition to being an intuitive and illustrative model of the reversible function of SERCA, this scheme is also able to describe the dependence of calcium uptake on SR calcium in a way that is valid not only in a normal myocyte, but also in circumstances in which the normal E–C coupling process is somehow disturbed. This has been established in previous studies of Shannon *et al.* (2000, 2004, 2005).

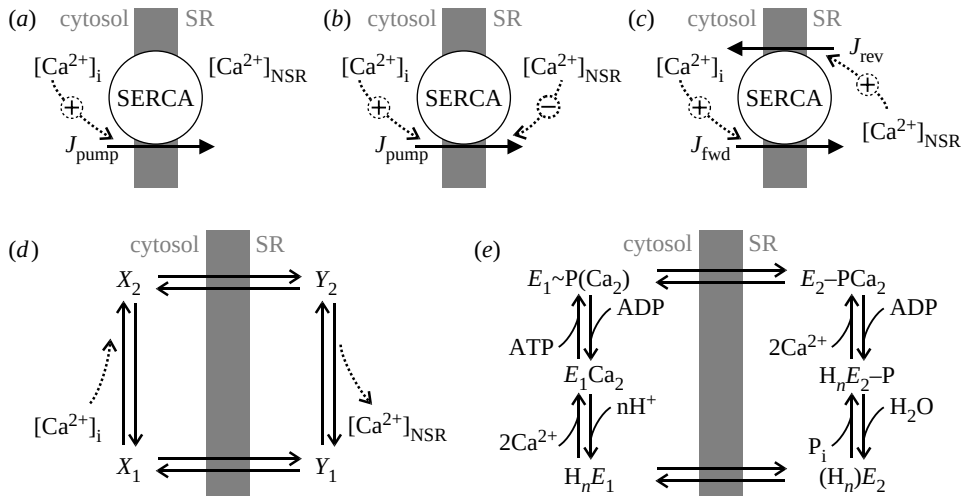

Figure 2. Schematics of SERCA models. (*a*) In the basic unidirectional pump model, calcium uptake is defined by the cytosolic calcium concentration $[Ca^{2+}]_i$ (see equation (2.1)). (*b*) The slightly more sophisticated model takes into account the inverse relationship of calcium uptake to the calcium concentration in the network SR $[Ca^{2+}]_{NSR}$ (see equation (2.2)). (*c*) The reversible function of SERCA is explicated in the bidirectional pump model in which a higher $[Ca^{2+}]_{NSR}$ reduces the uptake flux. (*d*) The inherent calcium-buffering effect of SERCA is taken into account in the four-state kinetic model, in which the binding and transport of calcium are described as separate processes. (*e*) A six-step reaction cycle model includes: binding of two Ca^{2+} ions to the SERCA pump from the cytoplasm, phosphorylation of the pump by ATP, conversion from the E_1 (cytosolic high-affinity binding site) into the E_2 (luminal low-affinity binding site) conformation state, translocation of Ca^{2+} from the cytosol to the luminal side of the SR membrane, release of Ca^{2+} into the SR, dephosphorylation of the pump and conversion from the E_2 into the E_1 conformation state.

(*c*) *Models incorporating the buffering of calcium*

The bidirectional pump model (equation (2.3)) is still deficient, in the sense that it does not account for the calcium-buffering effect of SERCA. Since SERCA protein is abundant in cardiac myocytes, it is the second most important intracellular calcium buffer after troponin (Bers 2001). During recent years, complex kinetic SERCA models, which include the binding and release of calcium and the change of conformation powered by ATP, have been presented. Among these schemes are, for example, descriptions with two (Matsuoka *et al.* 2003; Higgins *et al.* 2006), four (MacLennan *et al.* 1997; Matsuoka *et al.* 2003; Higgins *et al.* 2006) and six transitional states (Dode *et al.* 2002; Stokes & Green 2003; Yano *et al.* 2004; figure 2), corresponding to various conformational states during the transport cycle.

The schematics of the first model that describes the calcium-buffering effect of SERCA (Higgins *et al.* 2006) are shown in figure 2*d*. It includes four transitions: (i) the binding of cytosolic calcium, (ii) the change of conformation, (iii) the release of calcium into the SR, and (iv) the return to the original conformation. From a purely modelling perspective, the four-state model is problematic due to the number of unknown parameter values. Higgins *et al.* (2006) avoided this

dilemma by presenting a reduced, two-state model, for which they were able to assign parameter values based on thermodynamic calculations. In the same process, however, the model schematics and equations lose much of their intuitiveness and clarity.

(*d*) *Modelling of regulation of SERCA*

Evidently, the kinase-dependent regulation of SERCA is essential for myocytes in adaptation to the prevailing circumstances, both as dependence on beating frequency and in hormonal regulation. To our knowledge, this issue has been addressed only in four modelling studies with the implementation of a dynamic SERCA regulation by either PKA (Saucerman *et al.* 2003) or CaMKII (Hund & Rudy 2004; Iribe *et al.* 2006; Livshitz & Rudy 2007). While all these investigations provide sophisticated mathematical descriptions of the regulation, based on experimental findings, none of them attempted to combine the modulatory effects of CaMKII and PKA.

3. Novel SERCA model with calcium buffering

In the following, we present a novel model of the function of SERCA, which takes into account the calcium-buffering effect. Our aim was to implement this feature and the modulation of SERCA via phosphorylation by the two key enzymes, CaMKII and PKA, in a way that is both simplified and intuitive from the modelling perspective (i.e. small number of experimentally determined parameters) and exhaustive in the sense that it agrees with the experimental findings of calcium transport and its regulation. The model describes the binding of calcium on the cytosolic side and release to the SR with only two reversible kinetic transitions (figure 3*a*).

We would like to emphasize the fact that this model can be considered as a phenomenological description of the function of SERCA, which bypasses the exact transitional/conformational change of the enzymes with their unknown rate constants (compare figure 2), but reproduces the physiology. The function of the novel SERCA model is defined with the equations below, with some theoretical considerations to justify its use. First, we describe the dynamic regulation of PLB by its phosphorylation (equation (3.1)). This is followed by the definition of the forward and reverse calcium affinities of SERCA (equations (3.2) and (3.3)), including the binding and release kinetics (equations (3.4)–(3.7)). Based on these, we then calculate the calcium fluxes from the cytosol to SERCA, and from SERCA to the network SR, as well as the amount of calcium bound to SERCA.

To describe the phosphorylation of PLB induced by CaMKII and PKA, we formulated the following phenomenological equation to calculate the proportion of unphosphorylated phospholamban (marked here PLB):

$$\frac{\mathrm{d(PLB)}}{\mathrm{d}t} = k_{\mathrm{plb,neg}}(\mathrm{PLB_{TOT}} - \mathrm{PLB}) - k_{\mathrm{plb,pos}}(\mathrm{CaMKII_{reg}} + \mathrm{PKA_{reg}})^2\mathrm{PLB}, \quad (3.1)$$

where $\mathrm{CaMKII_{reg}}$ and $\mathrm{PKA_{reg}}$ are the relative regulatory activities of the respective enzymes (similarly in equations (3.2), (3.4) and (3.6)); $\mathrm{PLB_{TOT}}$ is the total amount of PLB (i.e. the sum of phosphorylated and unphosphorylated PLB); and the

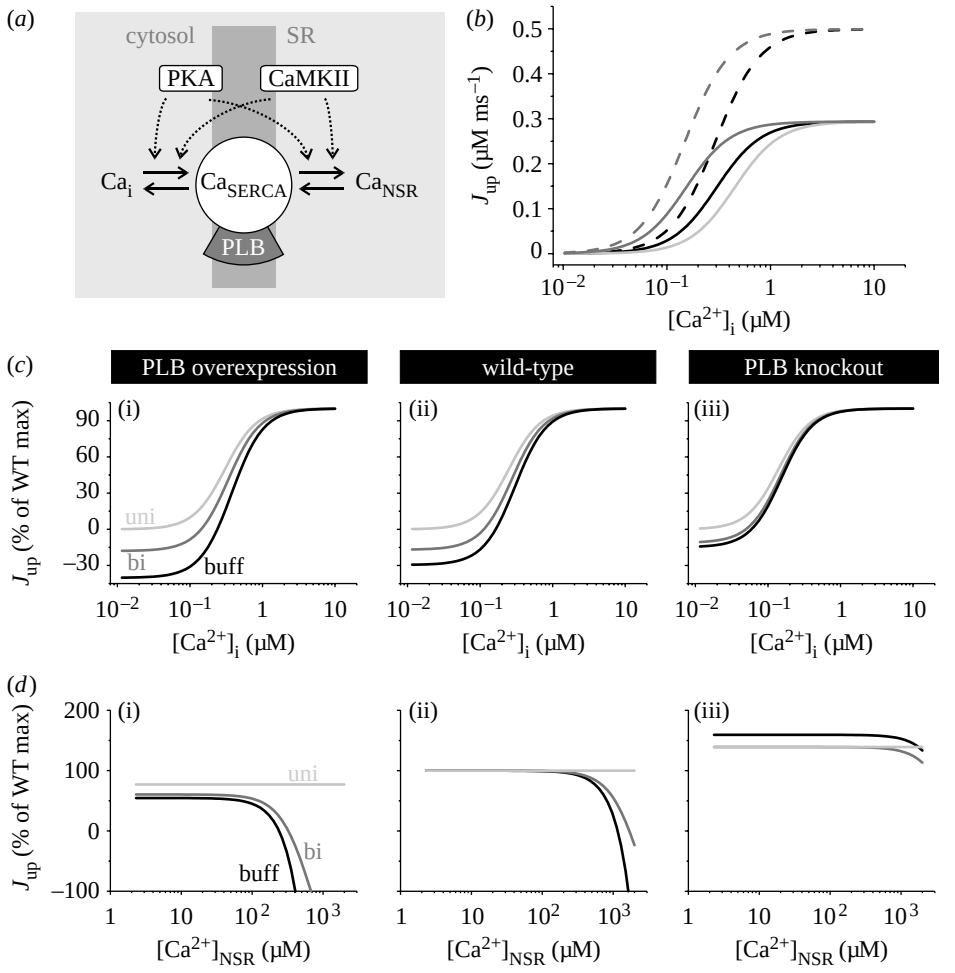

Figure 3. Schematics of the novel SERCA model and comparison of characteristics of the three models. (*a*) In the buffering SERCA model, calcium is taken up by SERCA from the cytosol and released into the network SR. Phosphorylation of PKA and CaMKII sites enhances the reaction kinetics. (*b*) SERCA is regulated by direct CaMKII phosphorylation and indirect phosphorylation of PLB at Ser16 and Thr17 sites by PKA and CaMKII, respectively. Direct phosphorylation of SERCA increases the maximum velocity of calcium uptake (dashed curves), and the amount of unphosphorylated PLB changes the EC_{50} value. Black, dark grey and light grey solid curves are for wild-type (WT), PLB knockout (PLBKO) and two-fold PLB overexpression (PLBOE), respectively. (*c*) Scaled calcium uptake is shown as a function of cytosolic calcium concentration, for three-model version: unidirectional, bidirectional and buffering. The SR calcium concentration was set to [532, 760, 988] μM for the PLBOE, WT and PLBKO test cases, respectively. (*d*) Scaled calcium uptake is shown as a function of SR calcium concentration. The cytosolic calcium concentration was set to [0.2, 0.25, 0.30] μM for the PLB overexpression, WT and PLBKO test cases, respectively. (*c*,*d*) (i) PLB overexpression, (ii) wild-type and (iii) PLB knockout.

kinetic parameters, $k_{\mathrm{plb,neg}}$ and $k_{\mathrm{plb,pos}}$, define the dephosphorylation and phosphorylation rates (see table 1 for numerical values). With first-order kinetics, the combined basal activities of PKA and CaMKII would result in rather a high baseline phosphorylation level of PLB. This is not expected on the

Table 1. Model parameters.

symbol	description	value
C_{m}	specific membrane capacitance	1.0 μF cm^{-2}
F	Faraday constant	96.5 C mmol^{-1}
T	temperature	298 K
R	universal gas constant	8.314 J K^{-1} mol^{-1}
A_{cap}	capacitive membrane area	1.534×10^{-4} cm^2
V_{myo}	myoplasmic volume	25.84×10^{-6} μl
$[\mathrm{Na}^+]_{\mathrm{o}}$	extracellular Na^+ concentration	140×10^3 μM
$[\mathrm{Na}^+]_{\mathrm{i}}$	intracellular Na^+ concentration	14×10^3 μM (short); 8.9×10^3 μM (long)
$[\mathrm{Ca}^{2+}]_{\mathrm{o}}$	extracellular Ca^{2+} concentration	1×10^3 μM
PSR	phospholamban to SERCA ratio	1 (for WT)
$\mathrm{PLB}_{\mathrm{TOT}}$	total amount of PLB	1 (relative value)
$k_{\mathrm{plb,pos}}$	rate of PLB phosphorylation	1 ms^{-1}
$k_{\mathrm{plb,neg}}$	rate of PLB dephosphorylation	6.8 ms^{-1}
$\mathrm{br}_{\mathrm{serca-nsr}}$	binding/release rate of calcium from SERCA to network SR	0.00625 ms^{-1}
$\mathrm{br}_{\mathrm{cyt-serca}}$	binding/release rate of calcium from cytosol to SERCA	$1000\times\mathrm{br}_{\mathrm{serca-sr}}$
$\mathrm{SERCA}_{\mathrm{TOT}}$	total amount of SERCA	47 μM (short); 20 μM (long)
k_{NCX}	scaling factor of $\mathrm{Na}^+/\mathrm{Ca}^{2+}$ exchange current	375 pA pF^{-1} (short); 1500 pA pF^{-1} (long)
$K_{\mathrm{m,Na}}$	Na^+ half-saturation constant	87.5 μM
$K_{\mathrm{m,Ca}}$	Ca^{2+} half-saturation constant	1.38 μM
k_{sat}	saturation factor at very negative potentials	0.1
η	voltage dependence control parameter	0.35
$\mathrm{CaM}_{\mathrm{TOT}}$	total myoplasmic calmodulin concentration	50.0 μM (uni and bi); 24.0 μM (buff)
$K_{\mathrm{m,CaM}}$	Ca^{2+} half-saturation constant for calmodulin	2.38 μM
$k_{\mathrm{LTRPN,pos}}$	Ca^{2+} on rate constant for troponin low-affinity sites	0.1 $\mu\mathrm{M}^{-1}$ ms^{-1}
$k_{\mathrm{LTRPN,neg}}$	Ca^{2+} off rate constant for troponin low-affinity sites	0.06 ms^{-1}
$\mathrm{LTRPN}_{\mathrm{TOT}}$	total low-affinity site troponin concentration	70.0 μM
$V^{\mathrm{O}}_{\mathrm{max}}$	basal maximum pump rate of SERCA	0.16 μM $(\mathrm{lcyt})^{-1}$ ms^{-1} (short) 0.10 μM $(\mathrm{lcyt})^{-1}$ ms^{-1} (long)
ν_2	Ca^{2+} leak rate constant from the NSR	$0.75\times1.74\times10^{-5}$ ms^{-1}
$k_{\mathrm{LTRPN,pos}}$	Ca^{2+} on rate constant for troponin low-affinity sites	30×0.00237 $\mu\mathrm{M}^{-1}$ ms^{-1}
$k_{\mathrm{LTRPN,neg}}$	Ca^{2+} off rate constant for troponin low-affinity sites	2×0.04 ms^{-1}
k_{NCX}	scaling factor of $\mathrm{Na}^+/\mathrm{Ca}^{2+}$ exchange current	2.5×125 pA pF^{-1} (short)
G_{Cab}	background Ca^{2+} current conductance	0.93×0.000367 mS $\mu\mathrm{F}^{-1}$

basis of the experimental findings, which indicate that stimulation of either PKA (Kadambi *et al.* 1996) or CaMKII (Hagemann *et al.* 2000) drastically enhances the pumping function of SERCA over baseline. Furthermore, either PKA or CaMKII alone can maximally phosphorylate PLB and thus fully relieve its inhibitory effect on SERCA (Chu *et al.* 2000; Hagemann *et al.* 2000). To attain an accurate description of the functionality under both baseline and maximal (phosphorylatory) stimulations, the square of the second term on the right-hand side of the equation is needed in equation (3.1).

The principle of bidirectional pumping function of SERCA was adapted from the scheme published by Shannon *et al.* (2000); see §2*b* for further reference. The numeric values of the affinities (EC_{50}^{fwd} and EC_{50}^{rev}) of the forward and reverse calcium fluxes (equations (3.2) and (3.3) below) were derived from previously published results (Bers 2001; Shannon *et al.* 2001, 2004) with the addition of dependence on the PLB to SERCA ratio (PSR) according to Luo *et al.* (1994), Kadambi *et al.* (1996), Chu *et al.* (1997), Brittsan *et al.* (2000), Frank *et al.* (2000) and Shannon *et al.* (2001). This formalism was chosen so that the model parameters could be linked easily to the values that are obtained from the analysis of experimental results. The affinities of the forward and reverse calcium fluxes are given by

$$EC_{50}^{fwd} = (0.15 + 0.15\ \mathrm{PSR\ PLB})(1 + 0.27\ \mathrm{CaMKII_{reg}}), \tag{3.2}$$

$$EC_{50}^{rev} = (2500 - 1110\ \mathrm{PSR\ PLB}). \tag{3.3}$$

For example, in the forward direction, the PSR dependence means that increased PLB expression decreases the calcium affinity of SERCA (increases the EC_{50} value), but this difference can be abolished with maximal phosphorylation of PLB, as has been observed in experiments (Kadambi *et al.* 1996). Measurements also indicate that phosphorylation of PLB does not have an effect on the maximum pump current (Toyofuku *et al.* 1994; Hagemann *et al.* 2000). Therefore, the last term in (3.2) is introduced to separate the effect of PLB phosphorylation from the direct phosphorylation of SERCA by CaMKII.

The binding and release kinetics of SERCA are calculated as simple first-order binding reactions

$$k_{\mathrm{cyt-serca}} = \mathrm{br_{cyt-serca}}(1 + 0.7\ \mathrm{CaMKII_{reg}}), \tag{3.4}$$

$$k_{\mathrm{serca-cyt}} = \mathrm{br_{cyt-serca}}\left(EC_{50}^{fwd}\right)^2, \tag{3.5}$$

$$k_{\mathrm{serca-sr}} = \mathrm{br_{serca-sr}}(1 + 0.7\ \mathrm{CaMKII_{reg}}), \tag{3.6}$$

$$k_{\mathrm{sr-serca}} = \frac{\mathrm{br_{serca-sr}}}{(EC_{50}^{rev})^2}, \tag{3.7}$$

where the ratio of $\mathrm{br_{cyt-serca}}$ to $\mathrm{br_{serca-sr}}$ was set to 1000, corresponding to the fact that calcium binding to SERCA is fast and the rate-limiting step in calcium uptake is the actual translocation of calcium to the network SR (MacLennan *et al.* 1997). The CaMKII-dependent terms describe the direct phosphorylation of SERCA by CaMKII, which can increase the maximum pump current by 70 per cent (Toyofuku *et al.* 1994; Xu & Narayanan 1999).

Based on the parameters defined in equations (3.4)–(3.7) (values presented in table 1), the fluxes resulting from calcium binding to and release from SERCA are defined with the following equations as functions of calcium concentrations in the cytosol and network SR ($[Ca^{2+}]_i$ and $[Ca^{2+}]_{NSR}$):

$$J_{cyt-serca} = k_{cyt-serca}[Ca^{2+}]_i^2(SERCA_{TOT} - [Ca^{2+}]_{serca}) - k_{serca-cyt}[Ca^{2+}]_{serca}, \quad (3.8)$$

$$J_{serca-sr} = k_{serca-sr}[Ca^{2+}]_{serca} - k_{sr-serca}[Ca^{2+}]_{NSR}^2(SERCA_{TOT} - [Ca^{2+}]_{serca}), \quad (3.9)$$

where $SERCA_{TOT}$ is the total amount of SERCA protein (species dependent, values in table 1). Thus, the amount of calcium bound to SERCA is calculated as

$$\frac{d([Ca^{2+}]_{serca})}{dt} = J_{cyt-serca} - J_{serca-sr}. \quad (3.10)$$

To illustrate the effect that PLB expression and phosphorylation have on the calcium uptake by SERCA, we have simulated the model in five test cases (figure 3*b*). In these simulations, the SR calcium concentration is set to zero, which is the typical experimental setting when calcium uptake is measured *in vitro*. The ratio of PLB to SERCA defines the EC_{50} value (figure 3*b*, solid curves) as observed *in vivo* (Luo *et al.* 1994; Kadambi *et al.* 1996; Chu *et al.* 1997; Brittsan *et al.* 2000; Frank *et al.* 2000), and the direct phosphorylation of SERCA by CaMKII increases the maximal uptake rate (figure 3*b*, dashed curves) in line with the experimental findings (Toyofuku *et al.* 1994; Xu & Narayanan 1999).

(*a*) *Characteristics of the three SERCA modelling approaches*

In order to compare the above-mentioned, both existing and novel modelling approaches, we calculated the calcium uptake in three test cases that have: (i) increased expression of PLB (PLBOE) by 50 per cent, (ii) normal PLB to SERCA ratio (wild-type, WT), and (iii) reduced expression of PLB (PLBKO). The resulting calcium fluxes (scaled to the corresponding WT maximum) are shown as functions of changing cytosolic (figure 3*c*) and network SR (figure 3*d*) calcium concentrations. In these two schemes, $[Ca^{2+}]_{NSR}$ and $[Ca^{2+}]_i$ were fixed to [532, 760, 988] μM and [0.2, 0.25, 0.30] μM, respectively. These three values correspond to PLBOE, WT and PLBKO as representative steady-state averages at 1 Hz pacing in a mouse cardiomyocyte.

As the first simulation scheme (figure 3*c*) with fixed $[Ca^{2+}]_{NSR}$ shows, the three models behave rather similarly, when the PLB to SERCA ratio is normal (figure 3*c*(ii)) or clearly reduced (figure 3*c*(iii)). However, the effect of reversible SERCA function is clearly demonstrated when the cytosolic calcium concentration is close to the diastolic value (approx. 0.1 μM). The deviation of the three modelling approaches is more apparent when PLB expression is increased (figure 3*c*(i)). This impedes the ability of SERCA to take up calcium against the existing gradient in the bidirectional and buffering models, but only to a lesser extent in the unidirectional model.

In a living cardiac myocyte, the calcium uptake flux is probably never reversed. As $[Ca^{2+}]_{NSR}$ increases due to the (forward mode) pumping of SERCA, the net flux balances to zero at a certain point. This phenomenon has been illustrated in the studies of Shannon *et al.* (2000, 2004, 2005). The significance of

modelling the reversible function of SERCA would appear highly important when the PLB to SERCA ratio is increased above the normal level, a situation that may be common in heart failure conditions (for a review see MacLennan & Kranias 2003).

4. Cytosolic calcium cycling: effect of the SERCA modelling approaches

Calcium handling in a cardiomyocyte is an inherently complex process with numerous interdependencies. Subtle but fundamental issues cannot be easily comprehended using a model containing all the components in the cardiomyocyte. We chose a drastically reduced model for the evaluation and illustration of the different approaches to the function of SERCA, but we then tested the schemes with a more complete model as well (see below). The basic idea was to calculate the calcium fluxes with the AP and the calcium input to the cytosol 'clamped' to have a fixed time course (analogously to voltage clamp). The reduced model has a single compartment that corresponds to the bulk cytosol of a myocyte (figure 4*a*). Within this compartment, the calcium changes are defined by (i) a fixed calcium input (combined SR release and L-type calcium flux), (ii) calcium removal by NCX and SERCA, (iii) calcium binding to troponin, and (iv) calcium buffering (mainly attributed to calmodulin). Extracellular calcium and sodium concentrations are considered to be constant (see table 1). The same applies for the network SR calcium concentration and intracellular sodium concentrations; during a normal AP cycle, they fluctuate only minimally. We find that the clamped AP and calcium inputs are very useful for the isolation of the effects that SERCA has on intracellular calcium. This kind of simulation approach has been used, for example, to study the coupling of AP and calcium transient during alternans (Livshitz & Rudy 2007).

To account for and to elucidate the species-specific differences, we have used two sets of parameters, which correspond to short (mouse) and long (guinea-pig) APs, for the NCX and SERCA. We also formulated two sets of inputs for the APs and calcium fluxes to the cytosol (figure 4*b*), using analytical functions suitable for this purpose (i.e. they do not change at all during the simulations with the reduced model; equations (A 1)–(A 4)).

(*a*) *Dynamics of calcium transients*

The reduced calcium cycling model enabled us to study the three SERCA modelling approaches in isolation from the other calcium transport mechanisms. As the trace in figure 4*c* shows, the reversible function and buffering feature of SERCA have only a small effect on the calcium transient. This is not surprising since the total amount of SERCA protein is not that large in myocytes with long AP. In this model, approximately 65 per cent of calcium is transported by the SERCA and 35 per cent by NCX. In the case of short AP, SERCA has a dominant role with a removal fraction of 90 per cent. Thus, it appears realistic that the inclusion of the buffering property of SERCA has a rather dramatic effect on the amplitude of calcium transients in the latter case (figure 4*d*).

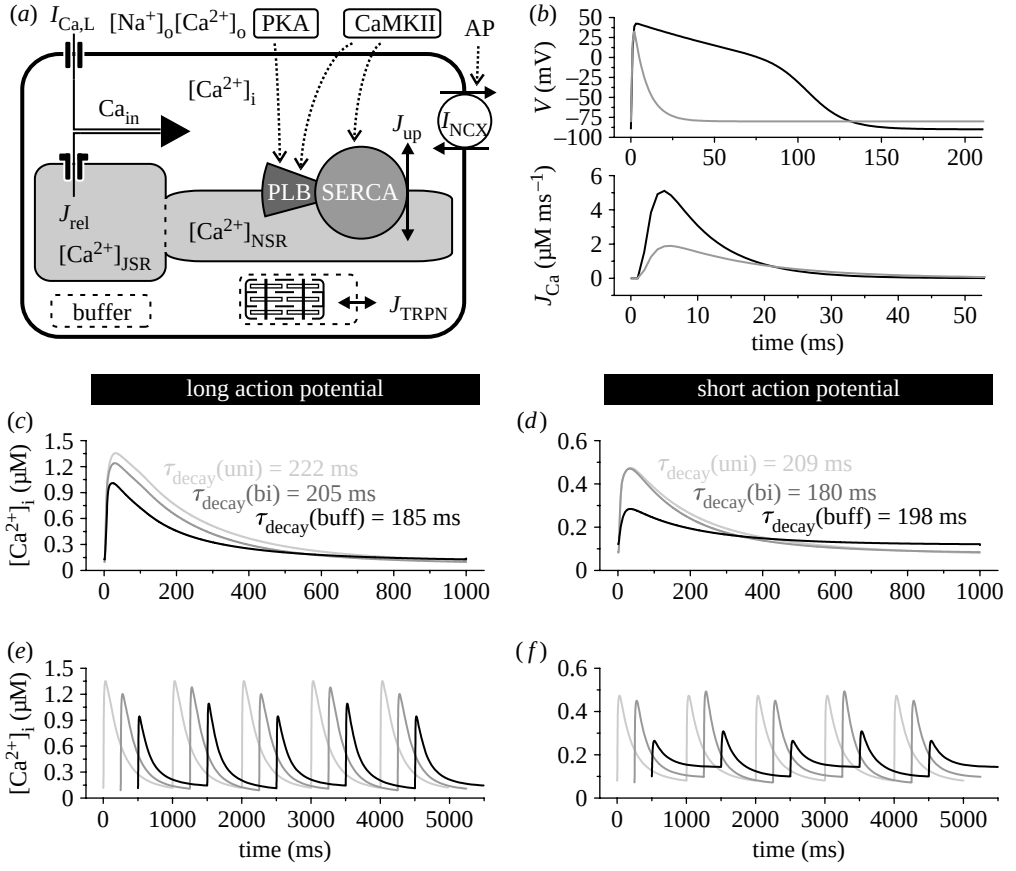

Figure 4. Model schematics and characteristics. (*a*) The reduced model of cytosolic calcium cycling includes the following components: calcium input (combined SR release, J_{rel}; and L-type calcium current, $I_{Ca,L}$), calcium extrusion by NCX (I_{NCX}), calcium uptake by SERCA (J_{up}) and calcium binding to troponin (J_{TRPN}). (*b*) Time traces of the AP and calcium input are shown for both the long (black) and short (grey) AP test cases. (*c*,*d*) Except for the variation in the amplitude, the calcium transients have the same dynamics. (*e*,*f*) A varying SR calcium concentration produces 'calcium alternans' in both of the reversible pump models, but not in the unidirectional model. (*c*,*e*) Long AP, (*d*,*f*) short AP; (*c*,*d*) steady-state calcium transient; (*e*,*f*) calcium transients—variable $[Ca^{2+}]_{NSR}$.

(*b*) *Physiological relevance: modelling calcium alternans*

The beat-to-beat alternation of the intracellular calcium transient could play a key role in the development of AP duration alternans (for a review see Weiss *et al.* 2006). Both experimental and theoretical studies have demonstrated that alternans is promoted when the fraction of calcium released from the SR has a steep dependence on (i) SR calcium load (Diaz *et al.* 2004), (ii) calcium-mediated refractoriness of SR release channels (Picht *et al.* 2006), or (iii) the sensitivity of SR calcium release channels (Diaz *et al.* 2002, 2004; Tao *et al.* 2008). The complexity of the phenomenon was elegantly pointed out by the recent in-depth studies of Xie *et al.* (2008), who proposed that intracellular calcium alternans depend, in a cooperative fashion, on SR calcium release, uptake and passive leak.

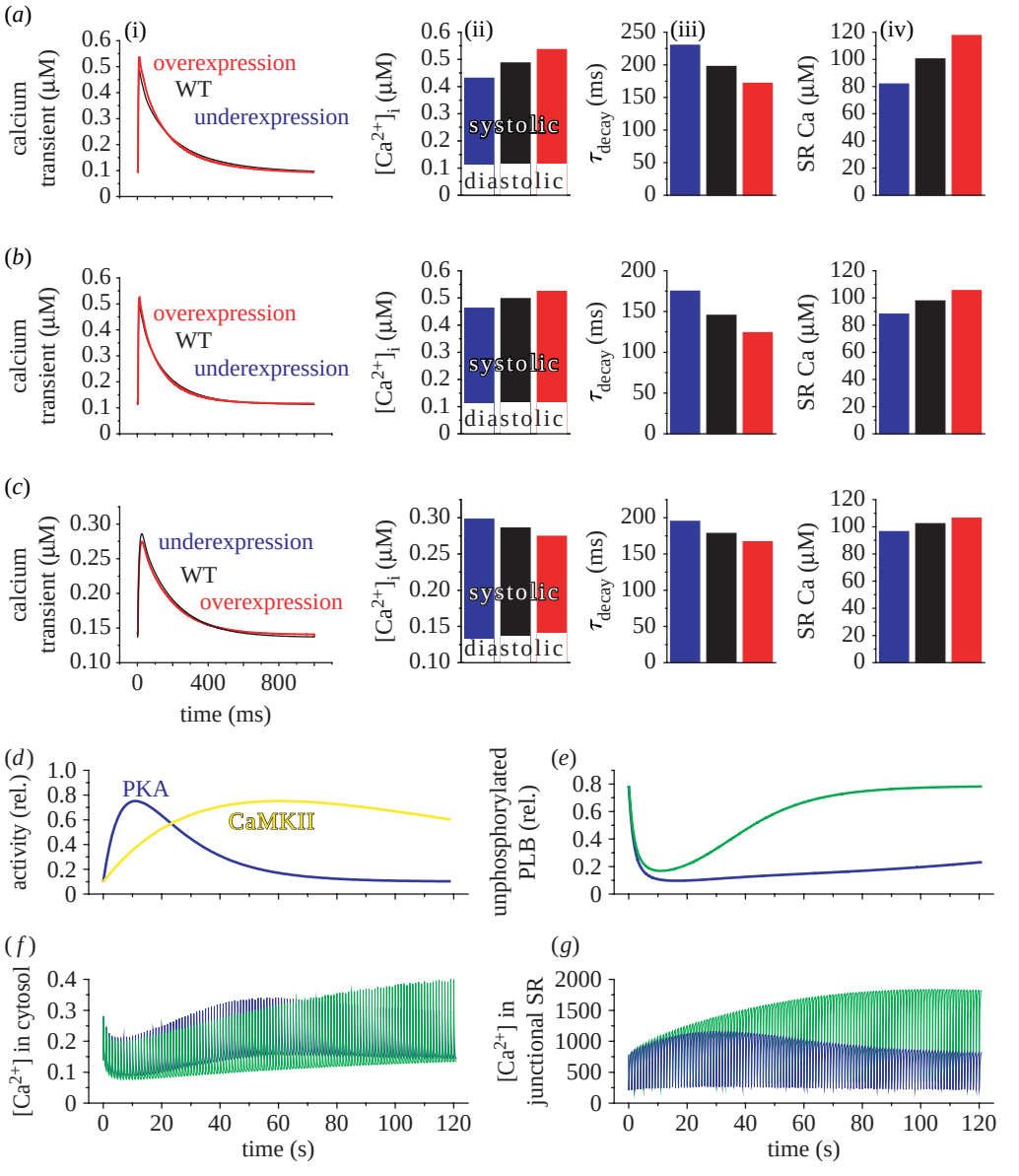

Figure 5. (*Caption opposite.*)

To demonstrate with the reduced model that the reversible function of a SERCA model is relevant in simulation studies of cardiac physiology, we calculated the steady-state calcium transients in a situation where $[Ca^{2+}]_{NSR}$ is increased and decreased by 20 per cent in every consecutive AP cycle (figure 4*e*,*f*). Both the bidirectional and buffering SERCA models reproduce alternating calcium transients, whereas the unidirectional model predicts a constant pattern. Thus, it would seem that a sophisticated SERCA model is an essential component, if the quantitative contribution of the various mechanisms promoting calcium alternans is to be elucidated further in simulations studies.

Figure 5. (*Opposite.*) Impact of the SERCA modelling approaches at whole-cell level. The effect of overexpression (red) and underexpression (blue) of SERCA by 20% compared with WT (black) is shown for all three cases: (*a*) unidirectional, (*b*) bidirectional and (*c*) buffering SERCA models. Results were obtained from steady-state simulations at 1Hz pacing. ((*a–c*)(ii) (iii)) For the uni- and bidirectional pump models, the increase in SERCA expression produces an expected effect: the amplitude of the calcium transient increases and the decay time constant decreases; however, in the case of the buffering SERCA model, the situation is slightly more complicated: increased SR calcium content and faster decay would tend to enhance E–C coupling, but the decreasing amplitude of the transient has an opposite effect. (*d*) Quasi-dynamic traces of PKA (blue) and CaMKII (yellow) activities (rel.) that were used as stimulation inputs. (*e–g*) Resulting changes of either bare PKA (blue) or combined PKA and CaMKII (green) activation on the cellular calcium dynamics in simulations that were started from a 1Hz pacing steady state. PLB phosphorylation promotes calcium uptake to the SR, and thus increased amplitude of calcium transient.

5. SERCA modelling in E–C coupling: myocyte simulations

To validate the buffering SERCA model further, we implemented (see appendix A for details) it into an existing mathematical model of mouse ventricular myocyte (Bondarenko *et al.* 2004), which includes membrane ionic channel currents, pumps and exchangers, and accounts for the processes that regulate intracellular concentration changes of Na^+, K^+ and Ca^{2+}.

(*a*) *Physiological impact of buffering SERCA model: transgenic test case*

As changes in the expression and the activity of SERCA are likely to contribute to cardiac dysfunction in a variety of pathological conditions (for a review see Periasamy *et al.* 2008), it was tempting to find out whether we could discover some differences in the predictions made with the three SERCA modelling approaches under conditions where the expression of the pump protein is either below or above the normal level. For this purpose, we implemented three versions of the E–C coupling model: (i) WT, (ii) 20 per cent overexpression (SERCAoe), and (iii) 20 per cent underexpression. For the sake of simplicity, we chose to change the amount PLB accordingly, i.e. the PLB to SERCA ratio stays constant.

Results of the simulations are shown in figure 5*a–c*. Since SERCA is a major regulator of the dynamics of calcium transients, even a subtle increase in the expression level should lead to an enhanced calcium removal from the cytosol and increased amount of calcium stored in the SR; and an opposite effect should be observed in the reduced expression of SERCA. Indeed, we did find that these changes take place with all three modelling approaches. The simulations thus offer one more level of validation for the novel buffering SERCA model. However, the results also point out a phenomenon that, at first glance, appears counter-intuitive. Contrary to the other two models, the buffering SERCA model predicts that increasing the pump protein expression decreases the amplitude of the calcium transient. More pumping capacity should lead to an increased calcium pool in the SR, and, further, to an increased calcium release, which should produce a larger calcium transient. In the simulations using the new model, the

first two are indeed increased compared with WT : SR calcium content by 4 per cent (figure 5*c*(iii)) and calcium release by 3 per cent (data not shown), but the amplitude of the transient is decreased by 10 per cent. The answer to this apparent paradox is the buffering function of SERCA, with the overexpression adding significantly to the total cytosolic buffering capacity. This means that at the initial phase of AP cycle, when calcium is released to the cytosol, more calcium is bound to SERCA (integral during first 50 ms: 19.0 and 20.9 μM for WT and SERCAoe, respectively). However, during the latter part of the cycle, the situation is reversed (18.8 and 18.4 μM for WT and SERCAoe, respectively), because SERCA is pumping against an increased gradient. Thus, during diastole, a larger amount of calcium remains to the cytosol (consequence of SR leak), which increases diastolic $[Ca^{2+}]_i$. A decreased amplitude of the calcium transient would of course mean a weaker contraction. Hence, a series of events of this sort could be one explanation why the efforts to improve the function of a failing heart with SERCA overexpression have produced contradictory results in various transgenic animal models (for a review see Vinge *et al.* 2008).

(*b*) *Dynamic regulation of SERCA*

To demonstrate the effects of dynamic and combined regulations of SERCA by PKA and CaMKII, we simulated the results shown in figure 5*e–g*. The time courses of quasi-dynamic regulatory activities of PKA and CaMKII (figure 5*d*) have been estimated based on the available literature (Wegener *et al.* 1989; Karczewski *et al.* 1990; Tavi *et al.* 2003; Iancu *et al.* 2007; see equations (A 14) and (A 15) for details). The combined activation of PKA and CaMKII, which corresponds to β-adrenergic stimulation with consequent activation of CaMKII, produces a fast phosphorylation of PLB (figure 5*e*, green line), which results in an increased calcium uptake (initial decrease in cytosolic calcium; figure 5*f*, green line). As the SR calcium content builds up (figure 5*g*, green line), the amplitude of the calcium transient starts to increase. The bare activation of PKA, equivalent to β-adrenergic stimulation with CaMKII inhibition, results in faster changes of the same parameters (figure 5*e–g*, blue lines).

6. Conclusions and future directions

In this study, we have systematically reviewed the three principal solutions used for the modelling of (cardiac) SERCA. Our results indicate that while the unidirectional pump model may be fairly sufficient for modelling normal physiological states, the reversible function and calcium-buffering aspect of SERCA need to be taken into account when we aim to understand the role SERCA both under physiological and pathophysiological conditions. We have presented one possible tool suitable for this objective, which is computationally efficient. This is an especially important feature if such models are, for example, to be integrated to the large-scale descriptions that are currently being developed in the extensive efforts of the Physiome Project (Hunter *et al.* 2002). One further improvement would be to add the variable stoichiometry of the coupling of transported Ca^{2+} and ATP consumption (Johnson *et al.* 1985; Yu & Inesi 1995; Alonso *et al.* 2001).

As SERCA is one of the major energy consumers in cardiac myocytes (after the contractile system), understanding its function and regulation from the perspective of energy balance appears essential. Indeed, both the exact mechanisms of function and the modulation of SERCA have been the subject of numerous studies in cardiac research, including transgenic animal models. One obvious future aim will be to extend the knowledge of the detailed mechanisms to the hypertrophied and failing human heart (for a review see Frank *et al.* 2002), a task where computational and modelling approaches will be of great help.

The study was conducted according to the guidelines of the Finnish National Advisory Board on Research Ethics.

This work was supported by the Biocenter Oulu Graduate School, Academy of Finland (to P.T. and M.W.) and the Sigrid Juselius Foundation (to P.T.).

Appendix A

The presented mathematical models were implemented with Matlab and the simulation results were obtained by numerically integrating the model equations with a stiff ordinary differential equation solver method. Unless stated otherwise, all the presented results were obtained by letting the model simulations run as long as was needed for the model to reach steady state with a definite pacing frequency. The mathematical models may be downloaded as Matlab files from http://cc.oulu.fi/~mtw/SERCA_model_JK.

(*a*) *Simplified model of cytosolic calcium cycling*

The reduced model of calcium dynamics in a myocyte is defined by the following equations (for parameter values see table 1). The short and long AP inputs, as well as the calcium input fluxes shown in equations (A 1)–(A 4) have been estimated on the basis of published simulation data (Bondarenko *et al.* 2004; Livshitz & Rudy 2007; for graphical illustrations see figure 4). Equations for the NCX current and calcium buffering have been adapted from a previously published cardiomyocyte model (Bondarenko *et al.* 2004).

The short and long AP inputs:

$$V(\mathrm{mV}) = -80 + 150(1-\exp(-t/0.5))^2 \exp(-t/8), \tag{A 1}$$

$$V(\mathrm{mV}) = -90 + 135(1-\exp(-t/0.5))^2 \exp(-t/200)(1-t^{10}/(110^{10}+t^{10})). \tag{A 2}$$

Calcium inputs for short and long APs:

$$\mathrm{Ca_{in}} = 2.9(1-\exp(-(t-1.2)/1.5))^2 \exp(-(t-1.2)/14), \tag{A 3}$$

$$\mathrm{Ca_{in}} = 10(1-\exp(-(t-1.2)/1.5))^2 \exp(-(t-1.2)/7.5). \tag{A 4}$$

NCX:

$$I_{\mathrm{NCX}} = k_{\mathrm{NCX}} \frac{[\mathrm{Na}^+]_{\mathrm{o}}^3}{K_{\mathrm{m,Na}}^3 + [\mathrm{Na}^+]_{\mathrm{o}}^3} \frac{[\mathrm{Ca}^{2+}]_{\mathrm{o}}}{K_{\mathrm{m,Ca}} + [\mathrm{Ca}^{2+}]_{\mathrm{o}}} \times \frac{\frac{[\mathrm{Na}^+]_{\mathrm{i}}^3}{[\mathrm{Na}^+]_{\mathrm{o}}^3} \mathrm{e}^{\eta VF/RT} - \frac{[\mathrm{Ca}^{2+}]_{\mathrm{i}}}{[\mathrm{Ca}^{2+}]_{\mathrm{o}}} \mathrm{e}^{(\eta-1)VF/RT}}{1 + k_{\mathrm{sat}}\, \mathrm{e}^{(\eta-1)VF/RT}}. \tag{A 5}$$

Calcium buffer and calcium flux to low-affinity troponin:

$$B_{\mathrm{i}} = 1 + \left(\frac{\mathrm{CaM_{TOT}}\, K_{\mathrm{m,CaM}}}{(K_{\mathrm{m,CaM}} + [\mathrm{Ca}^{2+}]_{\mathrm{i}})^2} \right)^{-1}, \tag{A 6}$$

$$J_{\mathrm{LTRPN}} = k_{\mathrm{LTRPN,pos}} [\mathrm{Ca}^{2+}]_{\mathrm{i}} (\mathrm{LTRPN_{TOT}} - \mathrm{LTRPN}) - k_{\mathrm{LTRPN,pos}}\, \mathrm{LTRPN}. \tag{A 7}$$

Differential equations:

$$\frac{\mathrm{d}([\mathrm{Ca}^{2+}]_{\mathrm{i}})}{\mathrm{d}t} = B_{\mathrm{i}} (I_{\mathrm{NCX}} A_{\mathrm{cap}} / (2 V_{\mathrm{myo}} F) + J_{\mathrm{up}} + J_{\mathrm{leak}} + J_{\mathrm{LTRPN}} + \mathrm{Ca_{in}}), \tag{A 8}$$

$$\frac{\mathrm{d}(\mathrm{LTRPN})}{\mathrm{d}t} = k_{\mathrm{LTRPN,pos}} [\mathrm{Ca}^{2+}]_{\mathrm{i}} (\mathrm{LTRPN_{TOT}} - \mathrm{LTRPN}) - k_{\mathrm{LTRPN,pos}}\, \mathrm{LTRPN}. \tag{A 9}$$

The PKA- and CaMKII-dependent regulation of affinities and maximum currents of the unidirectional and bidirectional SERCA models (see equations (2.1) and (2.3)) are calculated from the following equations. The parameter values are listed in table 1.

$$\mathrm{EC}_{50} = 0.15 + 0.15\, \mathrm{PSR}\, \mathrm{PLB}, \tag{A 10}$$

$$\mathrm{EC}_{50}^{\mathrm{fwd}} = 0.15 + 0.15\, \mathrm{PSR}\, \mathrm{PLB}, \tag{A 11}$$

$$\mathrm{EC}_{50}^{\mathrm{rev}} = 2500 - 1110\, \mathrm{PSR}\, \mathrm{PLB}, \tag{A 12}$$

$$V_{\mathrm{max}} = V_{\mathrm{max}}^0 (1 + 0.7\, \mathrm{CaMKII_{reg}}). \tag{A 13}$$

(*b*) *Mouse ventricular myocyte model*

In the myocyte model, the applied stimulus was a current pulse (amplitude -80 pA pF^{-1} and length 0.5 ms) which was repeated according to the desired pacing frequency. To increase the pacing steady-state stability of the model, we changed the original stimulation scheme so that the stimulus current is carried by K^+ ions as suggested by Hund *et al.* (2001). This approach resolved the problem of chronic $[\mathrm{K}^+]_{\mathrm{i}}$ and $[\mathrm{Na}^+]_{\mathrm{i}}$ depletions and thus ensured that the simulation results could indeed be obtained at a pacing steady state. We also made some modifications to the parameters of NCX to correct the circulation fractions of calcium and to obtain a better overall fit to the physiological data of

mouse myocytes (Li *et al.* 1998; Maier *et al.* 2003; see table 1 for details). Original initial values were used in the simulations (Bondarenko *et al.* 2004).

Dynamic PKA and CaMKII regulatory activities:

$$\mathrm{PKA}_{\mathrm{reg}} = 0.1 + 2.0\exp(-t/18\,000)(1-\exp(-\mathrm{t}/12\,000)), \tag{A 14}$$

$$\mathrm{CaMKII}_{\mathrm{reg}} = 0.1 + 2.0\exp(-t/99\,000)(1-\exp(-\mathrm{t}/66\,000)). \tag{A 15}$$

References

Alonso, G. L., González, D. A., Takara, D., Ostuni, M. A. & Sánchez, G. A. 2001 Kinetic analysis of a model of the sarcoplasmic reticulum Ca-ATPase, with variable stoichiometry, which enhances the amount and the rate of Ca transport. *J. Theor. Biol.* **208**, 251–260. (doi:10.1006/jtbi.2000.2185)

Barry, D. M. & Nerbonne, J. M. 1996 Myocardial potassium channels: electrophysiological and molecular diversity. *Annu. Rev. Physiol.* **58**, 363–394. (doi:10.1146/annurev.ph.58.030196.002051)

Bers, D. M. 2001 *Excitation–contraction coupling and cardiac contractile force*, 2nd edn. Dordrecht, The Netherlands: Kluwer.

Bers, D. M. 2002 Cardiac excitation–contraction coupling. *Nature* **415**, 198–205. (doi:10.1038/415198a)

Blaustein, M. P. & Lederer, W. J. 1999 Sodium/calcium exchange: its physiological implications. *Physiol. Rev.* **79**, 763–854.

Bondarenko, V. E., Szigeti, G. P., Bett, G. C. L., Kim, S. & Rasmusson, R. L. 2004 Computer model of action potential of mouse ventricular myocytes. *Am. J. Physiol. Heart Circ. Physiol.* **287**, H1378–H1403. (doi:10.1152/ajpheart.00185.2003)

Brittsan, A. G., Carr, A. N., Schmidt, A. G. & Kranias, E. G. 2000 Maximal inhibition of SERCA2 Ca^{2+} affinity by phospholamban in transgenic hearts overexpressing a non-phosphorylatable form of phospholamban. *J. Biol. Chem.* **275**, 12 129–12 135. (doi:10.1074/jbc.275.16.12129)

Cartwright, E. J., Schuh, K. & Neyses, L. 2005 Calcium transport in cardiovascular health and disease—the sarcolemmal calcium pump enters the stage. *J. Mol. Cell Cardiol.* **39**, 403–406. (doi:10.1016/j.yjmcc.2005.04.007)

Chu, G., Dorn II, G. W., Luo, W., Harrer, J. M., Kadambi, V. J., Walsh, R. A. & Kranias, E. G. 1997 Monomeric phospholamban overexpression in transgenic mouse hearts. *Circ. Res.* **81**, 485–492.

Chu, G., Lester, J. W., Young, K. B., Luo, W., Zhai, J. & Kranias, E. G. 2000 A single site (Ser16) phosphorylation in phospholamban is sufficient in mediating its maximal cardiac responses to beta-agonists. *J. Biol. Chem.* **275**, 38 938–38 943. (doi:10.1074/jbc.M004079200)

Diaz, M. E., Eisner, D. A. & O'Neill, S. C. 2002 Depressed ryanodine receptor activity increases variability and duration of the systolic Ca^{2+} transient in rat ventricular myocytes. *Circ. Res.* **91**, 585–593. (doi:10.1161/01.RES.0000035527.53514.C2)

Diaz, M. E., O'Neill, S. C. & Eisner, D. A. 2004 Sarcoplasmic reticulum calcium content fluctuation is the key to cardiac alternans. *Circ. Res.* **94**, 650–656. (doi:10.1161/01.RES.0000119923.64774.72)

Diaz, M. E., Graham, H. K., O'Neill, S. C., Trafford, A. W. & Eisner, D. A. 2005 The control of sarcoplasmic reticulum Ca content in cardiac muscle. *Cell Calcium* **38**, 391–396. (doi:10.1016/j.ceca.2005.06.017)

DiFrancesco, D. & Noble, D. 1985 A model of cardiac electrical activity incorporating ionic pumps and concentration changes. *Phil. Trans. R. Soc. Lond. B* **307**, 353–398. (doi:10.1098/rstb.1985.0001)

Dode, L., Vilsen, B., Baelen, K., Wuytack, F., Clausen, J. D. & Andersen, J. P. 2002 Dissection of the functional differences between sarco(endo)plasmic reticulum Ca^{2+}-ATPase (SERCA) 1 and

3 isoforms by steady-state and transient kinetic analyses. *J. Biol. Chem.* **277**, 45 579–45 591. (doi:10.1074/jbc.M207778200)

Favre, C. J., Schrenzel, J., Jacquet, J., Lew, D. P. & Krause, K. 1996 Highly supralinear feedback inhibition of Ca^{2+} uptake by the Ca^{2+} load of intracellular stores. *J. Biol. Chem.* **271**, 14 925–14 930. (doi:10.1074/jbc.271.25.14925)

Frank, K., Tilgmann, C., Shannon, T. R., Bers, D. M. & Kranias, E. G. 2000 Regulatory role of phospholamban in the efficiency of cardiac sarcoplasmic reticulum Ca^{2+} transport. *Biochemistry* **39**, 14 176–14 182. (doi:10.1021/bi001049k)

Frank, K. F., Bölck, B., Brixius, K., Kranias, E. G. & Schwinger, R. H. G. 2002 Modulation of SERCA: implications for the failing human heart. *Basic Res. Cardiol.* **97**, I72–I78. (doi:10.1007/s003950200033)

Hagemann, D., Kuschel, M., Kuramochi, T., Zhu, W., Cheng, H. & Xiao, R. P. 2000 Frequency-encoding Thr17 phospholamban phosphorylation is independent of Ser16 phosphorylation in cardiac myocytes. *J. Biol. Chem.* **275**, 22 532–22 536. (doi:10.1074/jbc.C000253200)

Han, C., Tavi, P. & Weckstrom, M. 2002 Modulation of action potential by $[Ca^{2+}]_i$ in modeled rat atrial and guinea pig ventricular myocytes. *Am. J. Physiol. Heart Circ. Physiol.* **282**, H1047–H1054. (doi:10.1152/ajpheart.00573.2001)

Higgins, E. R., Cannell, M. B. & Sneyd, J. 2006 A buffering SERCA pump in models of calcium dynamics. *Biophys. J.* **91**, 151–163. (doi:10.1529/biophysj.105.075747)

Hiranandani, N., Raman, S., Kalyanasundaram, A., Periasamy, M. & Janssen, P. M. L. 2007 Frequency-dependent contractile strength in mice over- and under-expressing the sarcoplasmic reticulum calcium ATPase. *Am. J. Physiol. Regul. Integr. Comp. Physiol.* **291**, R30–R36. (doi:10.1152/ajpregu.00508.2006)

Hund, T. J. & Rudy, Y. 2004 Rate dependence and regulation of action potential and calcium transient in a canine cardiac ventricular cell model. *Circulation* **110**, 3168–3174. (doi:10.1161/01.CIR.0000147231.69595.D3)

Hund, T. J., Kucera, J. P., Otani, N. F. & Rudy, Y. 2001 Ionic charge conservation and long-term steady state in the Luo–Rudy dynamic cell model. *Biophys. J.* **81**, 3324–3331. (doi:10.1016/S0006-3495(01)75965-6)

Hunter, P., Robbins, P. & Noble, D. 2002 The IUPS human physiome project. *Pflugers Arch.* **445**, 1–9. (doi:10.1007/s00424-002-0890-1)

Iancu, R. V., Jones, S. W. & Harvey, R. D. 2007 Compartmentation of cAMP signaling in cardiac myocytes: a computational study. *Biophys. J.* **92**, 3317–3331. (doi:10.1529/biophysj.106.095356)

Inesi, G., Prasad, A. M. & Pilankatta, R. 2008 The Ca^{2+} ATPase of cardiac sarcoplasmic reticulum: physiological role and relevance to diseases. *Biochem. Biophys. Res. Commun.* **369**, 182–187. (doi:10.1016/j.bbrc.2007.11.161)

Iribe, G., Kohl, P. & Noble, D. 2006 Modulatory effect of calmodulin-dependent kinase II on sarcoplasmic reticulum Ca^{2+} handling and interval–force relations: a modelling study. *Phil. Trans. R. Soc. A* **364**, 1107–1133. (doi:10.1098/rsta.2006.1758)

Jafri, M. S., Rice, J. J. & Winslow, R. L. 1998 Cardiac Ca^{2+} dynamics: the roles of ryanodine receptor adaptation and sarcoplasmic reticulum load. *Biophys. J.* **74**, 1149–1168. (doi:10.1016/S0006-3495(98)77832-4)

Johnson, E. A., Tanford, C. & Reynolds, J. A. 1985 Variable stoichiometry in active ion transport: theoretical analysis of physiological consequences. *Proc. Natl Acad. Sci. USA* **82**, 5352–5356. (doi:10.1073/pnas.82.16.5352)

Kadambi, V. J., Ponniah, S., Harrer, J. M., Hoit, B. D., Dorn II, G. W., Walsh, R. A. & Kranias, E. G. 1996 Cardiac-specific overexpression of phospholamban alters calcium kinetics and resultant cardiomyocyte mechanics in transgenic mice. *J. Clin. Invest.* **97**, 533–539. (doi:10.1172/JCI118446)

Karczewski, P., Bartel, S. & Krause, E. 1990 Differential sensitivity to isoprenaline of troponin I and phospholamban phosphorylation in isolated rat hearts. *Biochem. J.* **266**, 115–122.

Kiriazis, H. & Kranias, E. G. 2000 Genetically engineered models with alterations in cardiac membrane calcium-handling proteins. *Annu. Rev. Physiol.* **62**, 321–351. (doi:10.1146/annurev.physiol.62.1.321)

Koss, K. L. & Kranias, E. G. 1996 Phospholamban: a prominent regulator of myocardial contractility. *Circ. Res.* **79**, 1059–1063.

Koss, K. L., Grupp, I. L. & Kranias, E. G. 1997 The relative phospholamban and SERCA2 ratio: a critical determinant of myocardial contractility. *Basic Res. Cardiol.* **92**, 17–24. (doi:10.1007/BF00794064)

Kuhlbrandt, W. 2004 Biology, structure and mechanism of P-type ATPases. *Nat. Rev. Mol. Cell Biol.* **5**, 282–295. (doi:10.1038/nrm1354)

Li, L., Chu, G., Kranias, E. G. & Bers, D. M. 1998 Cardiac myocyte calcium transport in phospholamban knockout mouse: relaxation and endogenous CaMKII effects. *Am. J. Physiol. Heart Circ. Physiol.* **274**, H1335–H1347.

Linz, K. W. & Meyer, R. 2000 Profile and kinetics of L-type calcium current during the cardiac ventricular action potential compared in guinea-pigs, rats and rabbits. *Pflugers Arch.* **439**, 588–599. (doi:10.1007/s004240050982)

Livshitz, L. M. & Rudy, Y. 2007 Regulation of Ca^{2+} and electrical alternans in cardiac myocytes: role of CAMKII and repolarizing currents. *Am. J. Physiol. Heart Circ. Physiol.* **292**, H2854–H2866. (doi:10.1152/ajpheart.01347.2006)

Luo, C. H. & Rudy, Y. 1994 A dynamic model of the cardiac ventricular action potential. I. Simulations of ionic currents and concentration changes. *Circ. Res.* **74**, 1071–1096.

Luo, W., Grupp, I. L., Harrer, J., Ponniah, S., Grupp, G., Duffy, J. J., Doetschman, T. & Kranias, E. G. 1994 Targeted ablation of the phospholamban gene is associated with markedly enhanced myocardial contractility and loss of beta-agonist stimulation. *Circ. Res.* **75**, 401–409.

MacLennan, D. H. & Kranias, E. G. 2003 Phospholamban: a crucial regulator of cardiac contractility. *Nat. Rev. Mol. Cell Biol.* **4**, 566–577. (doi:10.1038/nrm1151)

MacLennan, D. H., Rice, W. J. & Green, N. M. 1997 The mechanism of Ca^{2+} transport by sarco(endo)plasmic reticulum Ca^{2+}-ATPases. *J. Biol. Chem.* **272**, 28 815–28 818. (doi:10.1074/jbc.272.46.28815)

Maier, L. S., Zhang, T., Chen, L., DeSantiago, J., Brown, J. H. & Bers, D. M. 2003 Transgenic $CaMKII\delta_c$ overexpression uniquely alters cardiac myocyte Ca^{2+} handling: reduced SR Ca^{2+} load and activated SR Ca^{2+} release. *Circ. Res.* **92**, 904–911. (doi:10.1161/01.RES.0000069685.20258.F1)

Matsuoka, S., Sarai, N., Kuratomi, S., Ono, K. & Noma, A. 2003 Role of individual ionic current systems in ventricular cells hypothesized by a model study. *Jpn J. Physiol.* **53**, 105–123. (doi:10.2170/jjphysiol.53.105)

Meyer, M., Bluhm, W. F., He, H., Post, S. R., Giordano, F. J., Lew, W. Y. & Dillmann, W. H. 1999 Phospholamban-to-SERCA2 ratio controls the force–frequency relationship. *Am. J. Physiol. Heart Circ. Physiol.* **276**, H779–H785.

Niggli, V. & Sigel, E. 2008 Anticipating antiport in P-type ATPases. *Trends Biochem. Sci.* **33**, 156–160. (doi:10.1016/j.tibs.2007.12.005)

Periasamy, M. & Kalyanasundaram, A. 2007 SERCA pump isoforms: their role in calcium transport and disease. *Muscle Nerve* **35**, 430–442. (doi:10.1002/mus.20745)

Periasamy, M., Bhupathy, P. & Babu, G. J. 2008 Regulation of sarcoplasmic reticulum Ca^{2+} ATPase pump expression and its relevance to cardiac muscle physiology and pathology. *Cardiovasc. Res.* **77**, 265–273. (doi:10.1093/cvr/cvm056)

Picht, E., DeSantiago, J., Blatter, L. A. & Bers, D. M. 2006 Cardiac alternans do not rely on diastolic sarcoplasmic reticulum calcium content fluctuations. *Circ. Res.* **99**, 740–748. (doi:10.1161/01.res.0000244002.88813.91)

Saucerman, J. J., Brunton, L. L., Michailova, A. P. & McCulloch, A. D. 2003 Modeling β-adrenergic control of cardiac myocyte contractility *in silico*. *J. Biol. Chem.* **278**, 47 997–48 003. (doi:10.1074/jbc.M308362200)

Shannon, T. R. & Bers, D. M. 1997 Assessment of intra-SR free [Ca] and buffering in rat heart. *Biophys. J.* **73**, 1524–1531. (doi:10.1016/S0006-3495(97)78184-0)

Shannon, T. R., Ginsburg, K. S. & Bers, D. M. 2000 Reverse mode of the sarcoplasmic reticulum calcium pump and load-dependent cytosolic calcium decline in voltage-clamped cardiac ventricular myocytes. *Biophys. J.* **78**, 322–333. (doi:10.1016/S0006-3495(00)76595-7)

Shannon, T. R., Chu, G., Kranias, E. G. & Bers, D. M. 2001 Phospholamban decreases the energetic efficiency of the sarcoplasmic reticulum Ca pump. *J. Biol. Chem.* **276**, 7195–7201. (doi:10.1074/jbc.M007085200)

Shannon, T. R., Wang, F., Puglisi, J., Weber, C. & Bers, D. M. 2004 A mathematical treatment of integrated Ca dynamics within the ventricular myocyte. *Biophys. J.* **87**, 3351–3371. (doi:10.1529/biophysj.104.047449)

Shannon, T. R., Wang, F. & Bers, D. M. 2005 Regulation of cardiac sarcoplasmic reticulum Ca release by luminal [Ca] and altered gating assessed with a mathematical model. *Biophys. J.* **89**, 4096–4110. (doi:10.1529/biophysj.105.068734)

Sneyd, J., Tsaneva-Atanasova, K., Bruce, J. I., Straub, S. V., Giovannucci, D. R. & Yule, D. I. 2003 A model of calcium waves in pancreatic and parotid acinar cells. *Biophys. J.* **85**, 1392–1405. (doi:10.1016/S0006-3495(03)74572-X)

Sorrentino, V. & Rizzuto, R. 2001 Molecular genetics of Ca^{2+} stores and intracellular Ca^{2+} signalling. *Trends Pharmacol. Sci.* **22**, 459–464. (doi:10.1016/S0165-6147(00)01760-0)

Stokes, D. L. & Green, N. M. 2003 Structure and function of the calcium pump. *Annu. Rev. Biophys. Biomol. Struct.* **32**, 445–468. (doi:10.1146/annurev.biophys.32.110601.142433)

Tao, T., O'Neill, S. C., Diaz, M. E., Li, Y. T., Eisner, D. A. & Zhang, H. 2008 Alternans of cardiac calcium cycling in a cluster of ryanodine receptors: a simulation study. *Am. J. Physiol. Heart Circ. Physiol.* **295**, H598–H609. (doi:10.1152/ajpheart.01086.2007)

Tavi, P., Allen, D. G., Niemelä, P., Vuolteenaho, O., Weckström, M. & Westerblad, H. 2003 Calmodulin kinase modulates Ca^{2+} release in mouse skeletal muscle. *J. Physiol.* **551**, 5–12. (doi:10.1113/jphysiol.2003.042002)

Toyofuku, T., Curotto Kurzydlowski, K., Narayanan, N. & MacLennan, D. H. 1994 Identification of Ser38 as the site in cardiac sarcoplasmic reticulum Ca^{2+}-ATPase that is phosphorylated by Ca^{2+}/calmodulin-dependent protein kinase. *J. Biol. Chem.* **269**, 26 492–26 496.

Vangheluwe, P., Sipido, K. R., Raeymaekers, L. & Wuytack, F. 2006 New perspectives on the role of SERCA2's Ca^{2+} affinity in cardiac function. *BBA-Mol. Cell Res.* **1763**, 1216–1228. (doi:10.1016/j.bbamcr.2006.08.025)

Vinge, L. E., Raake, P. W. & Koch, W. J. 2008 Gene therapy in heart failure. *Circ. Res.* **102**, 1458–1470. (doi:10.1161/CIRCRESAHA.108.173195)

Wegener, A. D., Simmerman, H. K., Lindemann, J. P. & Jones, L. R. 1989 Phospholamban phosphorylation in intact ventricles. Phosphorylation of serine 16 and threonine 17 in response to beta-adrenergic stimulation. *J. Biol. Chem.* **264**, 11 468–11 474.

Weiss, J. N., Karma, A., Shiferaw, Y., Chen, P. S., Garfinkel, A. & Qu, Z. 2006 From pulsus to pulseless: the saga of cardiac alternans. *Circ. Res.* **98**, 1244–1253. (doi:10.1161/01.RES.0000224540.97431.f0)

Xie, L., Sato, D., Garfinkel, A., Qu, Z. & Weiss, J. N. 2008 Intracellular Ca alternans: coordinated regulation by sarcoplasmic reticulum release, uptake, and leak. *Biophys. J.* **95**, 3100–3110. (doi:10.1529/biophysj.108.130955)

Xu, A. & Narayanan, N. 1999 Ca^{2+}/calmodulin-dependent phosphorylation of the Ca^{2+}-ATPase, uncoupled from phospholamban, stimulates Ca^{2+}-pumping in native cardiac sarcoplasmic reticulum. *Biochem. Biophys. Res. Commun.* **258**, 66–72. (doi:10.1006/bbrc.1999.0579)

Yano, K., Petersen, O. H. & Tepikin, A. V. 2004 Dual sensitivity of sarcoplasmic/endoplasmic Ca^{2+}-ATPase to cytosolic and endoplasmic reticulum Ca^{2+} as a mechanism of modulating cytosolic Ca^{2+} oscillations. *Biochem. J.* **383**, 353–360. (doi:10.1042/BJ20040629)

Yu, X. & Inesi, G. 1995 Variable stoichiometric efficiency of Ca^{2+} and Sr^{2+} transport by the sarcoplasmic reticulum ATPase. *J. Biol. Chem.* **270**, 4361–4367. (doi:10.1074/jbc.270.9.4361)